Fabrication of an inverse photoemission spectrometer to study unoccupied electronic states

A. K. Shukla, S. Banik and S. R. Barman

We discuss the performance of an inverse photoemission spectrometer that has been recently fabricated in our laboratory. The photon detector is of band-pass type with acetone gas filling and CaF_2 window (acetone/CaF_2). We determine the optimal operating conditions of the detector to be 4 mbar acetone pressure and 745 ± 20 V anode voltage. At these operating conditions, the count rate is improved by a factor of three to what has been reported earlier by Funnemann and Merz. We show that unlike other gas-filled detectors, acetone/CaF_2 detector works in the proportional region. Its dead time is negligible and addition of multiplier gas like argon worsens its performance. The performance of this detector has been compared with an ethanol/MgF_2 detector. High count rate, reasonable resolution, negligible dead time, no requirement of multiplier or quench gas, satisfactory stability, and ease of handling make the acetone/CaF_2 detector an attractive candidate for use in inverse photoemission spectroscopy (IPES). A low-energy electron gun of Stoffel–Johnson type has been fabricated and the beam current profile has been determined as a function of electron kinetic energy. The IPES spectra of polycrystalline Ag and Ta are shown and compared with data in the literature. By fitting the IPES Fermi edge of Ag, we find the overall resolution of the spectrometer to be 0.55 eV and the band-pass of acetone/CaF_2 detector to be 0.48 eV FWHM.

Keywords: Electron gun, inverse photoemission, photon detector, unoccupied states.

In order to investigate the electronic structure of a solid, it is useful to know the nature of both the occupied and unoccupied states around the Fermi level (E_F). Inverse photoemission spectroscopy (IPES) has emerged as a powerful technique to study the unoccupied electron states[1–4]. Gas-filled band-pass Geiger–Müller (GM) type counters are generally used for photon detection in IPES because of their high efficiency, low cost and simple design[5–12]. McLean and co-workers have reported various gas/window combinations like ethanol/MgF_2, 1-propanol/MgF_2, etc. among which ethanol/MgF_2 was reported[11,12] to

have the best detector band-pass of 0.35 eV. Use of acetone/CaF_2 detector was proposed by Funnemann and Merz and has been used by them for different scientific studies[7,13]. They reported[7] that this detector has small dead time and a band-pass of 0.4 eV. However, detailed characteristics of this detector have not been reported in the literature. To the best of our knowledge, no other group has used acetone/CaF_2 detector until now and generally, acetone detector has been considered to be unstable. In this note, we describe the fabrication of an IPES spectrometer using acetone/CaF_2 photon detector. The designs of the photon detector and the electron gun are described in detail. The count rate obtained by us is about three times higher than that reported earlier[7]. We show that the acetone/CaF_2 detector works in the proportional region with about 5 μs dead time, which is negligible.

Design and construction

The design of the photon detector is based on the following operating principle: the high energy cut-off of the acetone/CaF_2 detector is due to the CaF_2 window that does not transmit photons with energy > 10.2 eV, while the threshold for the photoionization of acetone at 9.7 eV sets the low energy cut-off[14]. This determines the band-pass function and results[7] in a mean photon detection energy of 9.9 eV with a FWHM of 0.4 eV. Thus, 9.9 ± 0.2 eV photons can enter the detector to photoionize acetone. For ethanol/MgF_2 detector, MgF_2 provides the high energy transmission threshold (10.97 eV), while the photoionization threshold of ethanol (10.48 eV) provides the low pass. The resulting[11] mean detection energy is 10.89 ± 0.18 eV.

The detector assembly has a modular design consisting of a 250 mm long stainless steel cylindrical tube with inner diameter 17.8 mm and outer diameter 21.2 mm, welded to a double-sided DN40 CF flange (7 in Figure 1) with a through hole equal to the inner diameter of the tube (4). Another double-sided DN40 CF flange (10) with a similar through hole has two additional 6 mm diameter through holes drilled in the radial direction. Two 6 mm diameter stainless steel tubes of length 25 mm are welded to these radial holes, and on the other end, DN16 CF flanges (8, 9) are welded to these tubes. These are used as gas inlet (8) and outlet (9). The anode (6) is attached to a SHV feedthrough (14) mounted on another DN40 CF flange (13) by a barrel connector (11). The three DN40 CF flanges (7, 10, 13) are mounted together on a linear translator (not shown in Figure 1) using bolts of 55 mm length. The anode is a 1.6 mm diameter electropolished stainless steel wire and is held by two perforated teflon spacers (5) in the detector tube. High voltage is applied to the anode and the region around the SHV and the barrel connector has been properly shielded using a teflon sleeve (12). The mechanical fabrication has been done by Sanskar Udhyog, Indore. The UHV welding and electropolishing have been done at Centre for Advanced Technology, Indore, India. A 25 mm diameter, 2 mm thick CaF_2 window (1, MgF_2 for ethanol) sits on a viton O-ring (2) and is tightly pressed by a stainless steel cap (3) at the entrance of the detector. This isolates the detector from the UHV chamber. Use of viton O-ring ensures easy exchange of windows at the testing stage of the detector. MgF_2 and CaF_2 windows have been procured from B. Halle Nachfl GmbH, Germany and Mateck GmbH, Germany respectively.

The count rate increases with higher solid angle of detection. So the detector is brought as close as possible to the sample using the linear translator. In order to increase the count rate, in a subsequent design we have increased the solid angle using another detector tube of inner diameter 23 mm and have fixed the window to it with a high-temperature glue, without using the stainless steel cap. This increases the count rate by 20%. A fraction of the electric field from inside the detector tube could come out through the insulating window, that was confirmed by calculating the electric field outside the window with and without a mesh. Thus, we have used a fine gold mesh in front of the window to prevent distortion of the IPES spectra.

Spectroscopy-grade acetone (S.D. Fine Chemicals, India, purity 99.8% and Merck, Germany, purity 99.9%, Uvasol grade) is filled in a glass test-tube welded to a stainless steel DN16~CF flange (MDC, UK) and is connected through a leak valve (Polaron CVT, UK) to the detector. The gas line is flushed with acetone several times. Acetone vapour is then allowed to leak into the detector up to the desired pressure. The fill-gas pressures are measured by convectron gauge (Granville Phillips, USA; model 375) as uncorrected apparent N_2 pressures. For ethanol/MgF_2 detector, spectroscopy-grade ethanol (Les Alcools De Commerce Inc., Canada; purity 99.8%) was used as detection gas and Ar (Inox, India; purity 99.9995%) was used as multiplier gas. The gas line has been leak-checked with He using a residual gas analyser (Pfeiffer Vacuum, Germany) to ensure the purity of the fill-gases in the detector. A turbo pump and rotary pump (Pfeiffer Vacuum), were used for pumping the detector tube and gas line.

The experimental chamber has been designed by us and fabricated by Polaron CVT. The chamber is made of *m*-metal that provides effective shielding for the low-energy electrons from the earth's magnetic field and stray magnetic fields. The system is equipped with low energy electron diffraction (LEED) system and sputter ion gun (Specs GmbH, Germany). The sample manipulator (Vacuum Generators, UK) is vertically mounted and has both azimuthal and axial rotations. The

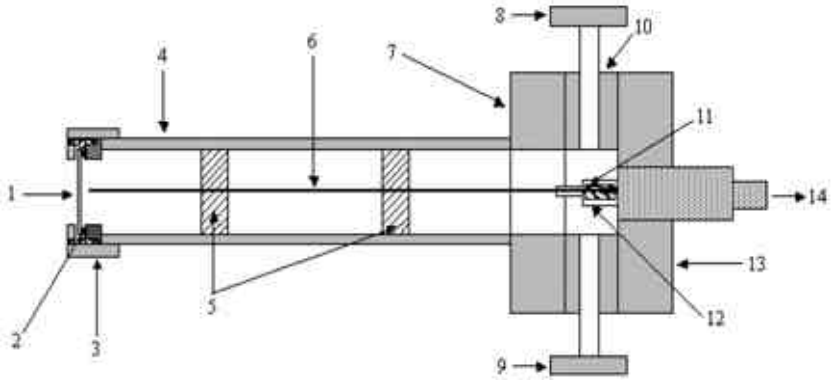

Figure 1. Schematic cross-section of the photon detector showing the window (1), O-ring (2), cylindrical cap (3), detector tube (4), teflon spacer (5), anode (6), double sided DN40 CF flanges (7, 10), gas inlet and outlet (8, 9), barrel connector (11), teflon sleeve (12), DN40 CF flange (13) and SHV connector (14).

base pressure in the experimental chamber is 5×10^{-11} mbar, which is measured using ionization gauge (Vacuum Generators).

The low-energy electron gun (e-gun) used in IPES has conflicting requirements of high intensity and good energy and momentum resolution. For low energy e-gun with high current density, space charge broadens the beam. We have fabricated a Stoffel Johnson (SJ)-type electron gun which has been designed specifically for IPES application[15]. SJ-type e-gun is chosen because it has less space-charge effect and high beam current. The minimum beam size obtained[15] for this gun is 1.1 mm, with full angular convergence of 5 to 7°. The design of the e-gun is schematically shown in Figure 2 *a*. The total length of the e-gun is about 49 mm and its outer diameter is 35 mm. It consists of a filament in a mounting block followed by three element lenses: extractor (A), focus (F) and output (O). All the lens elements are of cylindrical cross-section with 16 mm inner diameter. The electrical and mechanical spacing between the lenses is achieved by three sapphire balls of 3 mm diameter, located in the spherical grooves on each side of the elements. The e-gun is designed in such a way that the ceramic rod and the sapphire balls are not in the line-of-sight of the electrons, because this can cause the charging of the insulating surfaces leading to distortion of the electric field inside the gun. To obtain uniform work function over the whole surface area of the lenses, gold plating was done. We have used BaO dispenser cathode as the electron emitter. Figure 2 *b* shows the total beam current of the electron gun as a function of kinetic energy. In the low energy range from 6.5 to 10 eV, the beam current increases rapidly and then becomes almost constant for higher energies. The constant current level for higher energies is approximately ≈ 7 μA for the filament current of 0.22 A.

Data acquisition and control

Data acquisition and control is performed by a DAQ PCI 6024E card from National Instruments (NI), USA. It has 8 analogue voltage input channels, 8 digital-to-analogue converter (DAC) channels, 2 counter/timers, 8 digital I/O lines, etc. The card is installed in a Pentium III 700 MHz computer operating in Windows 2000 environment. Figure 3 shows the schematic layout of the data acquisition and control system for IPES. Voltages required for cathode and subsequent lens elements of electron gun are provided by a power supply, which requires 0–10 V input from the DAC channel of the DAQ card. The filament current for indirect heating of the BaO cathode is also provided from this power supply. The pulse counting electronics (Canberra, USA), comprises a charge sensitive pre-amplifier (model 2006), amplifier (model 2022) and a single-channel analyser (SCA, model 2030). All these modules are mounted in a NIM BIN power supply (ComTec GmbH, Germany). Charge pulses coming out of the detector are converted to voltage pulses by the preamplifier. These pulses are then fed to the amplifier, which has a variable gain (3–3000). Unipolar pulses at the amplifier output are fed to the SCA, which has lower and upper discriminator levels. The pulses which lie between the discriminator levels are converted into 5 V TTL pulses and are counted by the counter in the DAQ card. The upper discriminator level is set at 10 V. The lower discriminator level of the SCA is set above the noise level at 0.25 V. The dead count rate, i.e. counts with the electron gun switched-off is checked before measurement and is found to be negligible, typically 2–3 counts/s sr. The program for data acquisition and control has been written using LabVIEW 6.1 software (NI, USA). The flow chart of the program is shown in Figure 4. The data acquisition and control can be described in three parts: (i) setting of the kinetic energy E_j for the ith scan, (ii) acquisition of counts C_{ij} as a function of E_j and (iii) measurement of electron beam current (M_{ij}) through the sample. E_j can be set by providing a 0–10 V DAC output from the DAQ card to the electron gun power supply. For example, 1 V DAC output corresponds to 10 V cathode voltage, which produces electrons with E_j = 10 eV kinetic energy.

Detector optimization

The criteria for choosing the operating conditions of the acetone/CaF_2 detector are high count rate and good stability. The count rate has been determined at the Fermi edge of polycrystalline Ag as a function of acetone gas pressure (p) and anode voltage (V_A) (Figure 5 *a*). At each p, acetone has been refilled and the Ag sample has been sputtered so that the surface conditions are same for each p. V_A has been varied from 300 V until just

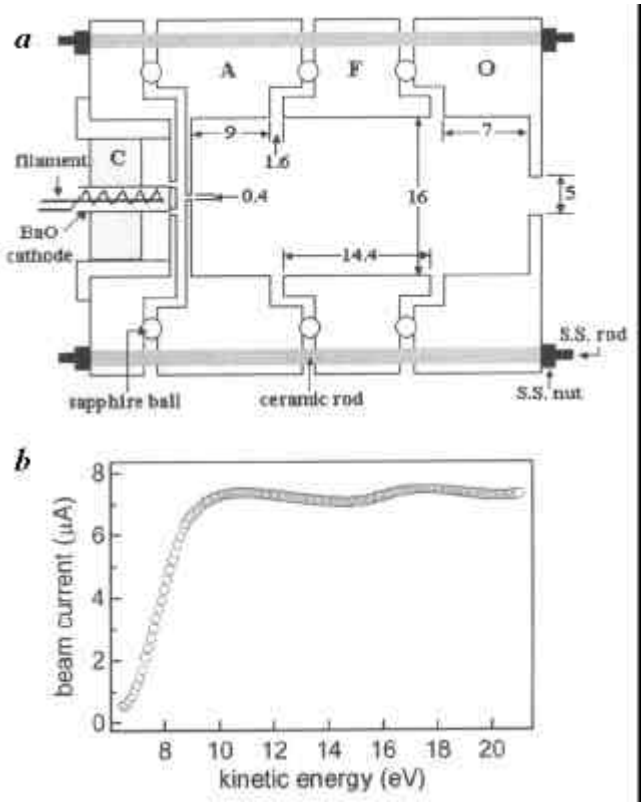

Figure 2. ***a***, Schematic cross-section of an electron gun of Stoffel–Johnson design. ***b***, Total beam current as a function of electron kinetic energy.

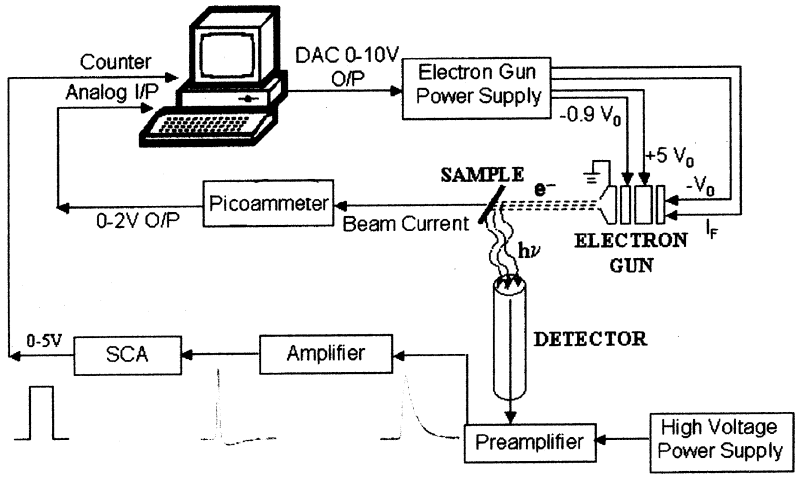

Figure 3. Layout of IPES data acquisition and control system.

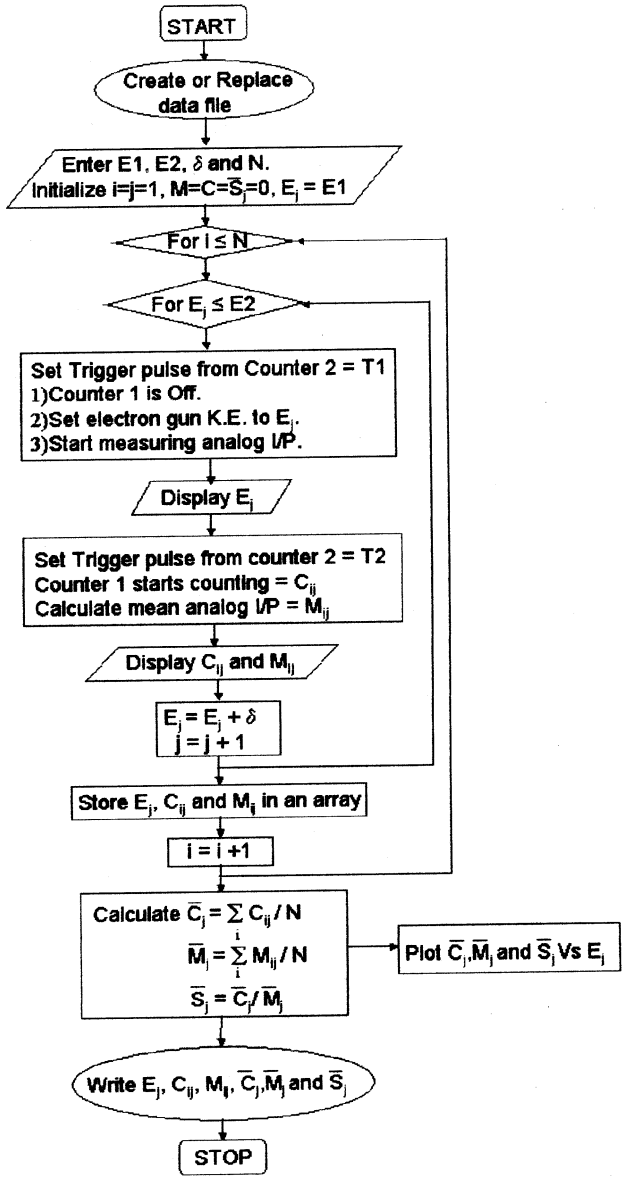

Figure 4. Flowchart for LabVIEW-based program for IPES data acquisition and control.

below the breakdown voltage (V_B). We find that the maximum count rate is obtained from about 3 mbar and 650 V to 6 mbar and 1050 V. As p is increased, V_A corresponding to maximum count rate (V_M) increases. The difference between V_B and V_M increases with p. In fact, V_B shows a steep increase for $p > 2$ mbar, as shown in Figures 5 *b*. This indicates that at higher acetone pressures the detector would be more stable. We choose the optimal operating condition where the count rate is maximum and V_B is considerably higher than V_M at $p = 4$ mbar, $V_M = 745 \pm 20$ V with V_B about 50 V higher[16]. However, counts decrease with time and after about 30–40 min stabilizes at 15–20% lower value. Considering this, the count rate that we obtain is about three times higher than that reported[7] earlier using $p = 0.75$ mbar.

Generally, inert gases like Ar or He are used as multiplier gas to facilitate the Geiger discharge[17]. For example, in ethanol/MgF_2 detector about 100 torr Ar is used with 1 torr ethanol[11]. Prince[9] used 100–150 mbar Ar in the dimethyl ether/MgF_2 detector. In the case of acetone/CaF_2, it has been reported that an admixture of He or Ar does not result in amplification of pulses[7]. Hence, we studied the behaviour of acetone/CaF_2 detector as a function of acetone + Ar pressure and V_A. Argon is introduced in the detector after filling it with 4 mbar acetone. Figure 5 *c* shows that the count rate decreases rapidly with increase in Ar partial pressure. Thus, Ar is actually detrimental for the operation of the acetone detector. Figure 5 *c* also shows how V_B varies with increasing Ar pressure. There is an initial rapid decrease from 800 to about 650 V, while above 8 mbar it increases to about 725 V.

Detector characteristics

In this section we study the characteristics of the acetone/CaF_2 detector. First, we find the average pulse height (m) as a function of the applied V_A. We have determined the average pulse height (m) for the acetone/CaF_2 detector at the output of the amplifier for $p = 4$ mbar (Figure 6). m shows an increase around 450 V, which can be taken as the onset voltage. Above 450 V, m exhibits almost a plateau, but increases gradually above 630 V. If we compare the variation of count rate (Figure 5 *a*) and m as a function of V_A, it is clear that above V_M although m increases,

the count rate decreases till the breakdown is reached (V_B = 800 V). We have also recorded *m* at other pressures (1 to 3 mbar) and find the behaviour to be similar, although the onset voltages, V_M and V_B, change. It is to be noted that the increase in *m* above 630 V indicates the start of the proportional region of operation in gas-filled detectors[17]. Thus, under normal operating conditions the acetone/CaF_2 detector works in the proportional region. In this region gas multiplication occurs, where the photoelectron liberated by photoionization is accelerated towards the anode by the applied voltage and produces additional electron–ion pairs by collision. The secondary electrons are also accelerated and produce subsequent ionization resulting finally in an avalanche[17]. We find that there is no need of any quench gas for the acetone detector, which is required for some gas-filled detectors working in the Geiger region[10]. Above 750 V, i.e. above V_M, the rapid increase in *m* indicates that the detector starts operating in the Geiger region. In this region of operation, ultraviolet photons created by the de-excitation of molecules start the avalanche process at different parts of the detector and ultimately the whole detector undergoes a Geiger discharge. However, the count rate of the acetone detector decreases in this region (Figure 5 *a*) and it becomes unstable, which shows that it is unable to sustain the Geiger process. Different fragmentation processes could be responsible for its instability[14,16]. When Ar is introduced, more electrons are emitted which facilitates more effective fragmentation. This causes both the count rate and V_B to decrease (Figure 5 *c*).

We find *m* to be about 1 V at V_M (Figure 6) from which the number of electrons in each pulse can be estimated to be about 10^4. In contrast, for the ethanol/MgF_2 detector studied by us, the number of electrons/pulse is 10^8. Thus the charge pulses in the acetone detector are four orders of magnitude less than in the ethanol detector. This also indicates the region of operation of the detectors. For proportional counters this number is between 10^2 and 10^4, while for GM counters[17] it is from 10^8 to 10^9. This further confirms that while the ethanol/MgF_2 detector works in the Geiger region, the acetone/CaF_2 detector operates in the proportional region. We have also recorded the count rate as a function of time by exposing the detector to an intense source of photons, i.e. the ionization gauge at a fixed filament current. We find that both detectors satisfy the relation that the standard deviation of the count rate is equal to the square root of the mean count rate. This observation indicates that both the detectors follow Poission distribution[17]. It should be noted that obeying Poission distribution does not necessarily mean Geiger operation[11], Geiger operation[11], since proportional counters also follow Poission statistics approximately[18].

In order to determine the dead time of the detectors, we show in Figure 7 the pulses at the amplifier output, where the first pulse has been triggered at time *t* = 0. This gives the behaviour of the pulses up to 500 μs after the appearance of the *t* = 0 pulse by repeated superposition for a long period (60 min) in the envelope mode of the CRO. For ethanol/MgF_2, no pulses are observed for about 100 μs after the *t* = 0 pulse, while after 100 μs, pulses of different height completely fill up the region so that the individual pulses cannot be distinguished. Although the IPES process occurs and countable photons are generated, the absence of pulses between 0 and 100 μs shows that the detector is unable to count for this time period. This is known as the dead time, as shown in Figure 7 *c*. Dead time results from reduction of the applied field in the detector due to positive space charge formed during Geiger discharge[5,8,10,11,17]. After the dead time, the detector starts to recover and produce pulses, although of smaller height compared to the *t* = 0 pulse. However, the pulse height increases exponentially as is evident from the envelope of the pulse heights (Figure 7 *c*), and the time constant of this exponential function is estimated by fitting to be 126 μs. This is known as the recovery time[11].

In contrast, the acetone/CaF_2 detector exhibits a different behaviour (Figure 7 *a*, *b*). As expected, immediately ('0' min) after starting the pulse recording, it shows no pulses after the *t* = 0 pulse (Figure 7 *a*). After 60 min, there are pulses of

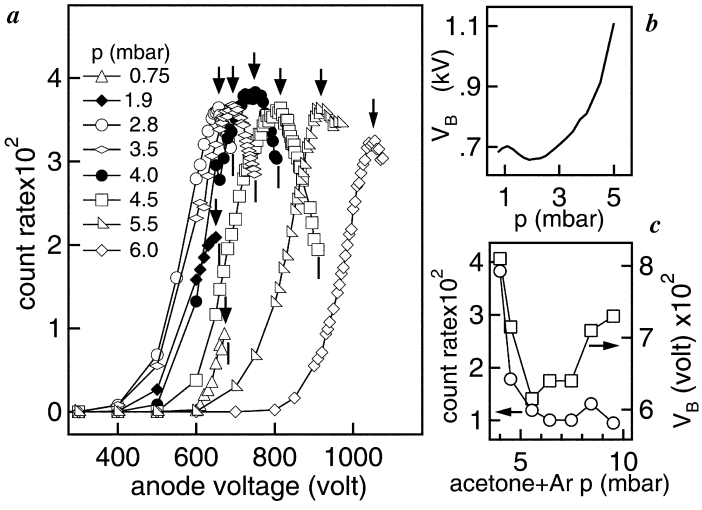

Figure 5. ***a***, Count rate (in counts/μA s sr) at Ag Fermi edge as a function of anode voltage at different acetone pressures (*p*). Voltage corresponding to the maximum counts (V_M) and breakdown voltage (V_B) is indicated by arrow and tick respectively. ***b***, Variation of V_B as a function of *p*. ***c***, Count rate at Ag Fermi edge (open circles) and V_B (open squares), as a function of acetone + Ar gas pressure for an initial filling of 4 mbar acetone.

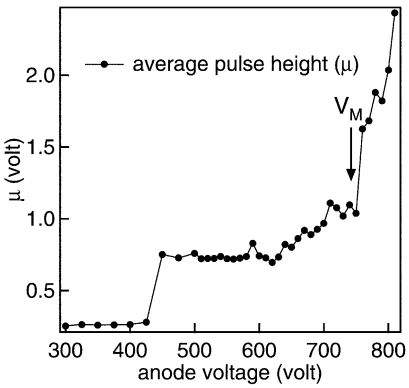

Figure 6. Average pulse height (*m*) of acetone/CaF_2 as a function of anode voltage at *p* = 4 mbar.

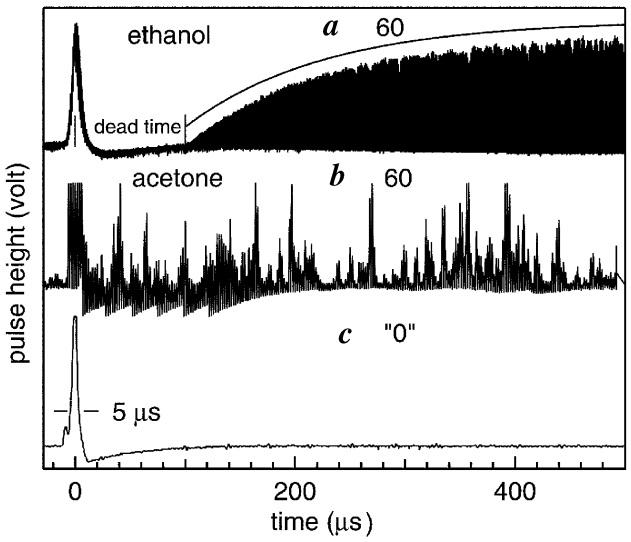

Figure 7. Pulses at output of the amplifier recorded in the envelope mode of the CRO after triggering the first pulse at $t = 0$ for (***a***, ***b***) acetone/CaF_2 and ethanol/MgF_2 (***c***). The time (in min) is indicated. For ethanol/MgF_2, the dead time is indicated and an exponential fit to the envelope is shown slightly staggered along the vertical axis.

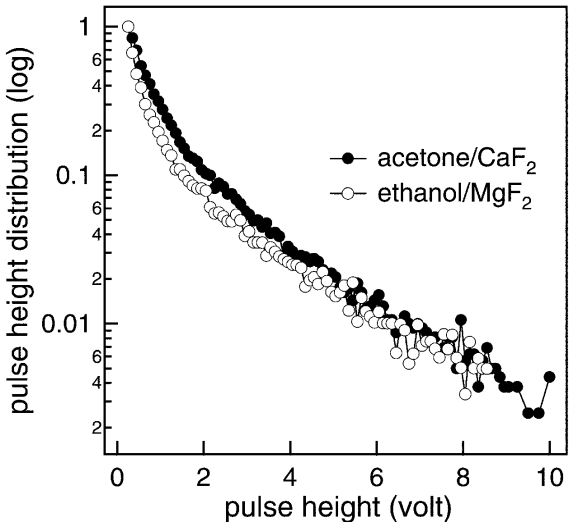

Figure 8. Pulse height distribution of acetone/CaF_2 (filled circle) and ethanol/MgF_2 (open circle).

different heights over the whole range, 0 to 500 μs. If acetone (Figure 7 *b*) and ethanol (Figure 7 *c*) detector envelopes are compared, it is clear that there is no signature of either dead time or recovery time in the former. So, in this case we estimate the dead time from the FWHM of the $t = 0$ pulse (Figure 7 *a*) to be about 5 ± 0.5 μs. This dead time is negligible and is typical for proportional counters[17].

The pulse height distribution (PHD) is a fundamental property of a detector that is routinely used to deduce information about its operation[17]. To determine the PHD, we recorded pulses at the output of SCA. The SCA has a window defined by lower (E, in volts) and upper (ΔE) discriminator levels, and pulses whose heights are within this window are counted. We have fixed ΔE at 0.1 V and varied E from 0.25 to 10 V in steps of 0.1 V. The count rates at each of these windows of width 0.1 V ($= \Delta E$) give the PHD shown in Figure 8. For the purpose of comparison, maximum of the PHD for both the detectors is normalized to unity. We find that the PHD of acetone decreases exponentially, as expected for proportional counters[7,18]. It is interesting to note that although ethanol detector operates in the Geiger region[11,16], its PHD turns out to be similar to the acetone detector. This is probably related to the operation of the ethanol detector during the recovery time, where pulses much smaller than the $t = 0$ pulse are also recorded as counts. It should be noted that for both the detectors, the lower discriminator level is kept same, i.e. just above the electronic noise level in order to maximize the count rate.

IPES spectra

Figure 9 shows polycrystalline Ag IPES spectrum recorded with the acetone/CaF_2 detector. The spectrum recorded by us is in good agreement with those from the literature[7]. In the near E_F region, the spectrum is dominated by the 5s and 5p-like states. Since the dead-time is negligible, no dead time correction is required unlike the ethanol detector[11]. The shape remains the same for spectra recorded at different p and anode voltages. For this reason the Ag spectrum recorded by Funnemann and Merz[7] at $p = 0.75$ mbar and 650 V agrees with our spectra recorded at $p = 4$ mbar and 745 V. To estimate the resolution of the spectrometer, Ag spectrum in the near E_F region has been recorded with small step size, 0.02 eV (inset, Figure 9 *a*). This has been fitted with a parameter-dependent function, which involves a spectral function multiplied by the Fermi function and this is convoluted with a resolution function which is approximated as a Gaussian[16]. From the fitting, we obtain the overall instrumental resolution to be 0.55 ± 0.007 eV, which is the FWHM of the Gaussian function. This resolution is in agreement with that in the literature (0.55 eV)[7]. As mentioned earlier, this shows that there is no significant change in resolution with the operating conditions. We determine the position of the Fermi level (shown by vertical line in the inset, Figure 9 *a*) to be 8.18 ± 0.001 eV also from the fitting. Assuming a Maxwellian distribution, the FWHM of the electron source can be taken to be about 0.26 eV at 1200 K operating temperature. Thus, the acetone detector band-pass FWHM can be calculated to be $\sqrt{(0.05)^2 - (0.26)^2} = 0.48$ eV. Figure 9 *b* shows the polycrystalline Ta IPES spectrum recorded with the acetone/CaF_2 detector, which is in good agreement with

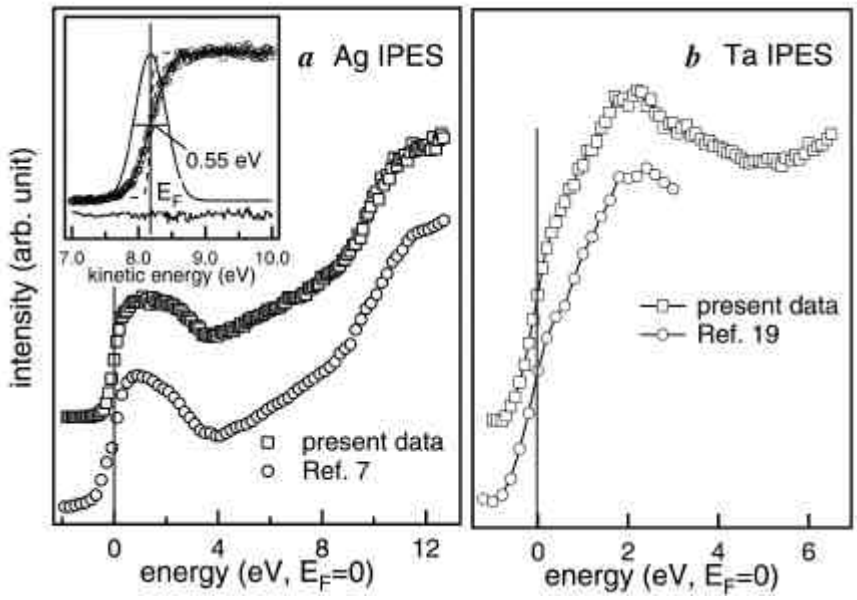

Figure 9. ***a***, IPES spectrum of Ag compared with that published in the literature. (Inset) IPES spectrum of Ag in the near E_F region (open circles) with fitted spectrum (thick solid line), Fermi function (dashed line) and instrumental Gaussian function (thin solid line). The residual is shown at the bottom. ***b***, IPES spectrum of Ta compared with that published in the literature. The Fermi level (vertical line) is defined as the zero of the energy scale. Spectra are staggered along the vertical axis.

the spectrum from the literature (A. B. McLean, unpublished, http: //www.physics/queensu.ca/nanophysics/inverse/spectra/spectra.html). Above E_F, the spectrum is dominated by unoccupied 4d states.

1. Dose, V., *Prog. Surf. Sci*., 1983, **13**, 225–284.
2. Smith, N. V., *Rep. Prog. Phys*., 1988, **51**, 1227–1294.
3. Johnson, P. D. and Hulbert, S. L., *Rev. Sci. Instrum*., 1990, **61**, 2277–2288.
4. Himpsel, F. J., *Surf. Sci. Rep*., 1990, **12**, 3–48.
5. Denninger, G., Dose, V. and Scheidt, H., *Appl. Phys. A*, 1979, **18**, 375–380.
6. Allen, P. M. G., Dobson, P. J. and Edgell, R. G., *Solid State Commun*., 1985, **55**, 701–704.
7. Funnemann, D. and Merz, H., *J. Phys. E: Sci. Instrum*., 1985, **19**, 554–557.
8. Dose, V., Fauster, Th. and Schneider, R., *Appl. Phys. A*, 1986, **40**, 203–207; Goldmann, A., Donath, M., Altmann, W. and Dose, V., *Phys. Rev. B*, 1985, **32**, 837–850.
9. Prince, K. C., *Rev. Sci. Instrum*., 1988, **59**, 741–742.
10. Hill, I. G. and McLean, A. B., *Rev. Sci. Instrum*., 1998, **69**, 261–264.
11. Lipton-Duffin, J. A., Mark, A. G. and McLean, A. B., *Rev. Sci. Instrum*., 2002, **73**, 3149–3154.
12. Lipton-Duffin, J. A., Mark, A. G., Mullins, G. K., Contant, G. E. and McLean, A. B., *Rev. Sci. Instrum*., 2004, **75**, 445–454.
13. Ostendorf, R., Wulff, K., Benesch, C., Merz, H. and Zacharias, H., *Phys. Rev. B*, 2004, **70**, 205325; Ostendorf, R., Benesch, C., Haquodorn, M., Merz, H. and Zacharias, H., *Phys. Rev. B*, 2002, **66**, 245401; Benesch, C., Merz, H. and Zacharias, H., *Phys. Rev. B*, 2002, **65**, 235317; Benesch, C., Fartmann, M. and Merz, H., *Phys. Rev. B*, 2001, **64**, 205314.
14. Trott, W. M., Blais, N. C. and Walters, E. A., *J. Phys. Chem*., 1978, **69**, 3150–3158.
15. Stoffel, N. G. and Johnson, P. D., *Nucl. Instrum. Methods Phys. Res. A*, 1985, **234**, 230–234.
16. Banik, S., Shukla, A. K. and Barman, S. R., *Rev. Sci. Instrum*., 2005, **76**, 066102.
17. Knoll, G. F., *Radiation Detection and Measurement*, Wiley, New York, 1989.
18. Campbell, J. L. and Ledingham, K. W. D., *Br. J. Appl. Phys*., 1966, **17**, 769–774.

ACKNOWLEDGEMENTS. The work was funded by Department of Science and Technology, New Delhi. Profs A. B. McLean, D. D. Sarma, K. Horn and Ms C. Biswas are thanked for useful discussions. Drs B. A. Dasannacharya, P. Chaddah and Prof. A. Gupta are thanked for continued support. Mr V. Bhatnagar, Mr S. C. Das and Mr Ramshankar are thanked for technical help.

Received 5 July 2005; revised accepted 23 November 2005

A. K. Shukla, S. Banik and S. R. Barman are in the UGC–DAE Consortium for Scientific Research, Khandwa Road, Indore 452 017, India*
**For correspondence.*
e-mail: barman@csr.ernet.in